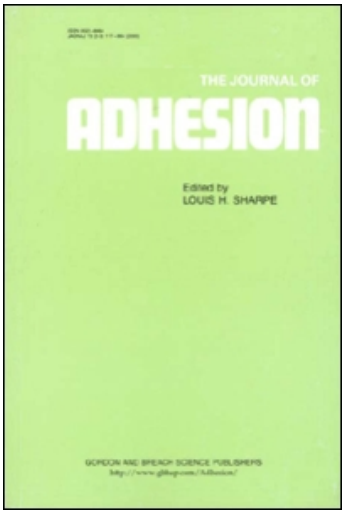

The Journal of Adhesion
Publication details, including instructions for authors and subscription information:
http://www.informaworld.com/smpp/title~content=t713453635

Evaluation of Fracture Surfaces in Carbon Fiber/Epoxy Composites

C-T. Chou[a]; U. Gaur[a]; B. Miller[a]
[a] TRI/Princeton, Princeton, New Jersey, U.S.A.

To cite this Article Chou, C-T. , Gaur, U. and Miller, B.(1993) 'Evaluation of Fracture Surfaces in Carbon Fiber/Epoxy Composites', The Journal of Adhesion, 40: 2, 245 — 256
To link to this Article: DOI: 10.1080/00218469308031287
URL: http://dx.doi.org/10.1080/00218469308031287

J. Adhesion, 1993, Vol. 40, pp. 245–256
Reprints available directly from the publisher
Photocopying permitted by license only

Printed in the United States of America.

Evaluation of Fracture Surfaces in Carbon Fiber/Epoxy Composites*

C.-T. CHOU, U. GAUR and B. MILLER

TRI/Princeton, P.O. Box 625, Princeton, New Jersey 08542, U.S.A.

(Received March 7, 1992; in final form June 4, 1992)

We have investigated carbon fiber/resin debonding mechanisms using wetting force scanning to examine the fracture surfaces. The wettability of the site of a resin microdroplet (50–150 μm long) on a fiber after debonding is compared with that of the original fiber surface by scanning along the fiber with an appropriate probe liquid. For an HMS/Epon828 system, debonding seems to involve removal of a layer of carbon fiber, while for an AS4/Epon828 system, there is evidence for adhesive failure as well as cohesive failures in both fiber and resin. These contrasting failure mechanisms are consistent with the morphological structures of the carbon fibers studied.

KEY WORDS composite; failure mechanism; fracture surface; wettability; interface; adhesion; debonding mechanisms; microdroplet; epoxy resin

INTRODUCTION

Most interpretations of interfacial shear strength measurements assume that adhesive failure has taken place at the interface during fiber/resin debonding. For nearly all cases, SEM observations of fiber surfaces after pullout experiments have not shown any resin residues, nor was there any evidence of fiber fibrillation. This implies that there is no gross cohesive failure in the resin or in the fiber. However, such SEM observations cannot eliminate the possibility of cohesive failure either in the resin or in the fiber at a depth less than the limits of SEM observation. Indeed, it has been reported that, for carbon fiber reinforced composites, the locus of bond failure may lie only several nanometers into the fiber surface or, in other words, that debonding involves cohesive failure between the skin of the carbon fiber and its core.[1-3]

We have recently started to investigate carbon fiber/resin debonding mechanisms by examining fracture surfaces using wetting force scanning. The wettability of the site of a debonded resin microdroplet (50–150 μm long) on a fiber is compared with that of the original fiber surface by scanning with an appropriate probe liquid. Different failure modes were observed for different carbon fiber/resin combinations.

*Presented at the Fifteenth Annual Meeting of The Adhesion Society, Inc., Hilton Head Island, South Carolina, U.S.A., February 17–19, 1992.

EXPERIMENTAL

Unsized HMS and AS4 carbon fibers with standard electrooxidation treatment (Hercules) were used in this study. Microcomposite specimens were prepared by depositing microdroplets of epoxy resin (Epon828®, Shell) on single filaments. The resin was then cured with methylene dianiline (weight ratio 4:1) at 80°C for 2 hours followed by 3 hours at 150°C.

To create a fracture surface, we used the TRI microbond pullout force instrumentation.[4] As shown in Figure 1, the fiber was pulled out from the matrix volume using a microvise consisting of two adjustable plates that form a slit which is attached to a vertical drive system. The plates are positioned just above the droplet, and the slit is narrowed symmetrically until the plates just make contact with the fiber. Then, as the plates move downward, they encounter the droplet and exert a downward shearing force on it. After debonding, the microdroplet is moved at least 500 μm away from the original location (see Figure 2). This provides a fiber specimen with a fracture surface at an identified location.

The fracture surface is then evaluated by comparing the wettability of the microdroplet site on the fiber with that of the original fiber surface. This is accomplished by scanning with an appropriate probe liquid using a technique based on the Wilhelmy wetting force principle.[5] As shown in Figure 3, the specimen is suspended vertically from the arm of a Cahn D-200 microbalance, while a precision elevator

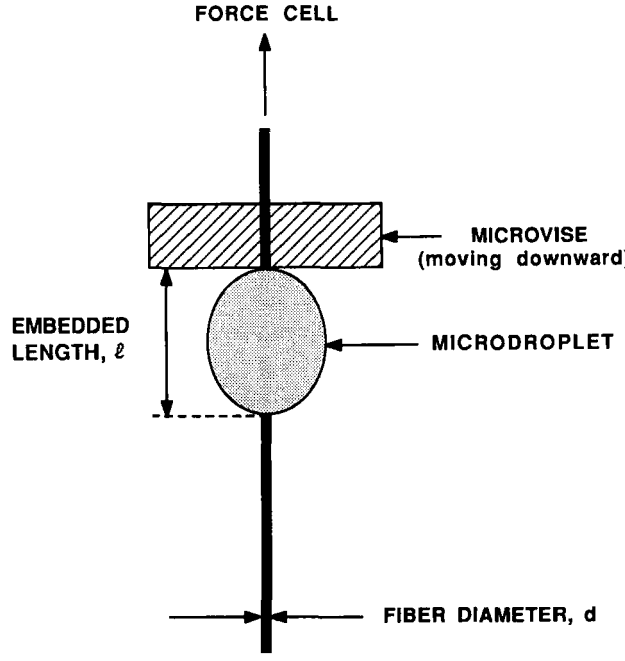

FIGURE 1 TRI Microbond specimen.

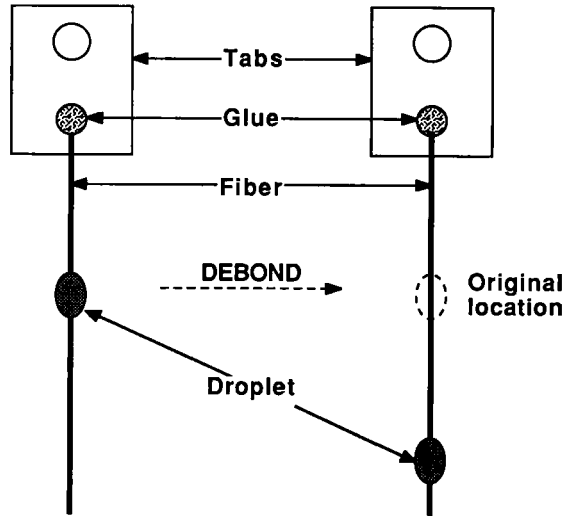

FIGURE 2 Fracture surface specimen preparation using microbond technique.

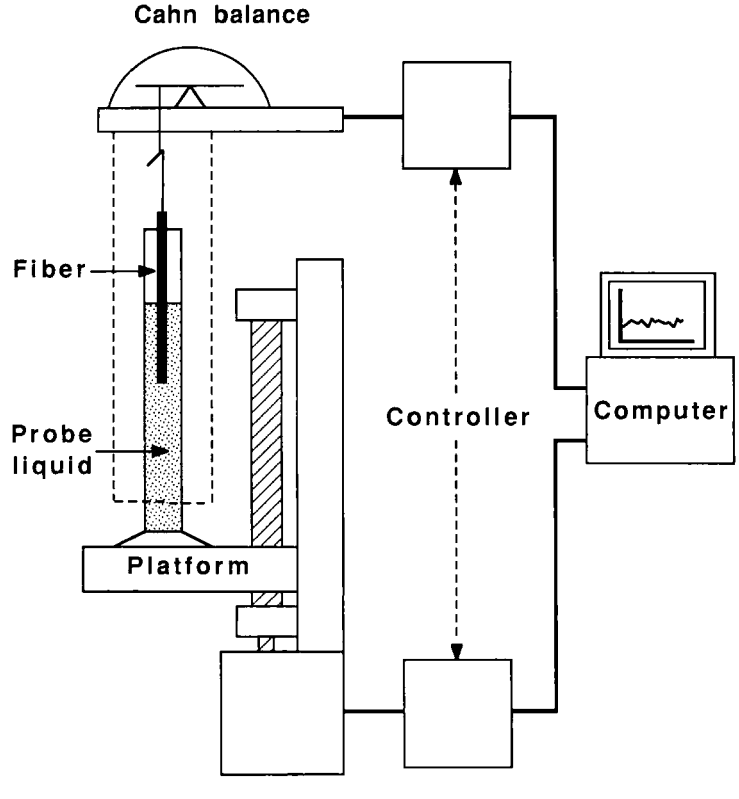

FIGURE 3 Wetting force measurement apparatus.

raises and lowers a liquid surface along the fiber. The scanning rate must be slow enough so that detail is not lost; the experiments reported were run at 1 μm/s along ~1000 μm of fiber. A computer periodically records the change in apparent weight caused by wetting forces at the three-phase boundary. The contact angle, θ, and work of adhesion, W, between the fiber and probe liquid at any location along the fiber length can be obtained using the following equations:

$$F = \gamma_L P \cos\theta \quad (1)$$

$$W = \gamma_L + \gamma_L \cos\theta \quad (2)$$

where γ_L is the surface tension of the probe liquid, F is the measured wetting force, and P is the specimen perimeter.

Ethylene glycol was used as the probe liquid. Its surface tension was determined using Equation 1 from wettability measurements on a platinum wire with a known perimeter and a zero-degree contact angle.

The procedure for fracture surface evaluation involves first scanning the microcomposite specimen with the microdroplet intact on the fiber. Due to large differences between the perimeters of the fiber and the microdroplet, this first scan provides the exact location of the microdroplet on the scan trace (a typical scan trace is shown in Figure 4). The first wetting force scan also reveals any variation of W along the fiber before debonding. After the microdroplet is displaced, the fiber specimen with the fracture surface at the identified location is then remounted on the wettability balance and rescanned. Since the entire fiber surface, with the exception of the microdroplet site, is now being scanned for a second time, whereas the fracture surface is being wetted for the first time, observed wettability differences between the two may reflect differences between virgin wetting and rewetting. For this reason, the specimen is scanned again, and the third scan is used to look for permanent wettability differences between the fiber and the fracture surface. To

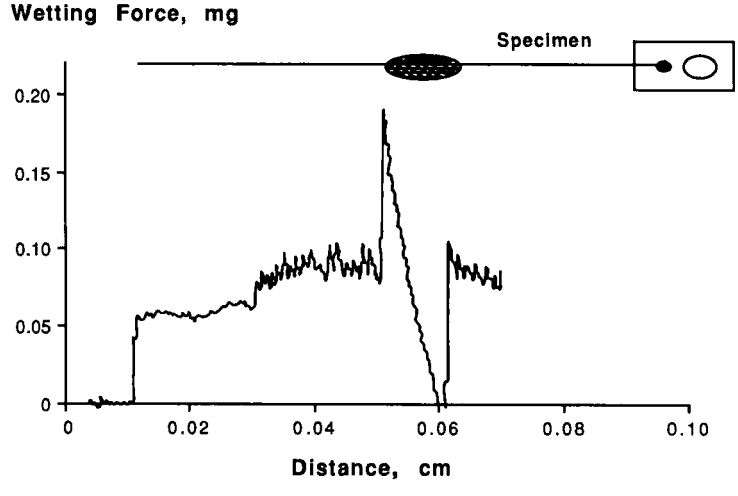

FIGURE 4 Advancing wettability for HMS/epoxy microbond specimen before debonding.

determine whether or not the perimeter of the specimen at the microdroplet site had changed significantly, the relevant sections of the fiber were rescanned with a surfactant solution of known surface tension γ_L. Since such a low energy liquid makes a zero-degree contact angle with the fiber, the measured wetting force F can be used to compute the perimeter: $P = F/\gamma_L$.

RESULTS AND DISCUSSIONS

HMS/epoxy

Figure 5 shows the results of the second and third advancing and receding scans for a HMS/Epon828 fracture surface in terms of work of adhesion W between the probe liquid and the fiber surface. The scans clearly show a significant drop in work of adhesion at the microdroplet site. The third scans for four other specimens are shown in Figure 6. In each case there is a well defined drop in W in the region of the fracture surface, particularly for the receding scans.

Typical perimeter scans for two of the specimens (Figure 7) illustrate that there are no detectable changes in specimen perimeter at the microdroplet site, indicating that gross cohesive failure has not taken place. This was further substantiated by SEM views of the fiber at the microdroplet site. The representative micrographs shown in Figure 8 illustrate that, although there were some random particulate residues on the fiber surface, there were no continuous deposits of resin and no evidence of fiber fibrillation.

The wettability data suggest that debonding the HMS/epoxy interface involves either removal of a layer of carbon fiber along with the resin microdroplet, or submicroscopic cohesive failure in the resin resulting in a thin residual layer of epoxy on the fiber (Figure 9). Since the core of the carbon fiber would be expected to have lower wettability than the electrooxidized surface, and the wettability of epoxy was

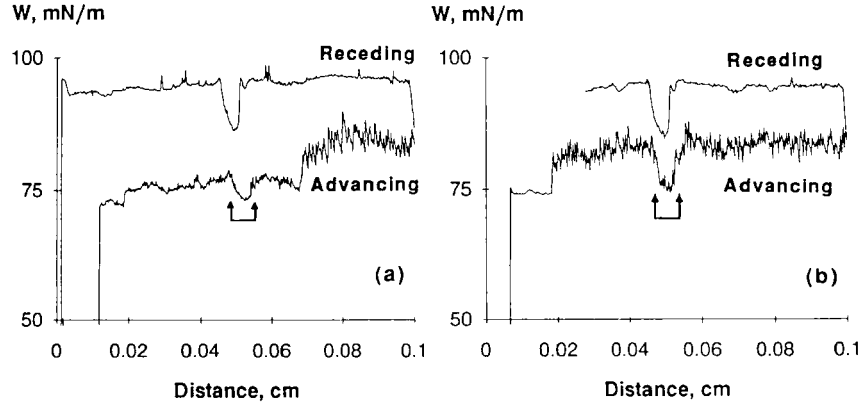

FIGURE 5 Second and third wettability scans along the HMS fiber of Figure 4 after debonding the Epon828® microdroplet. Note the decrease in W at the fracture surface indicated by arrows.

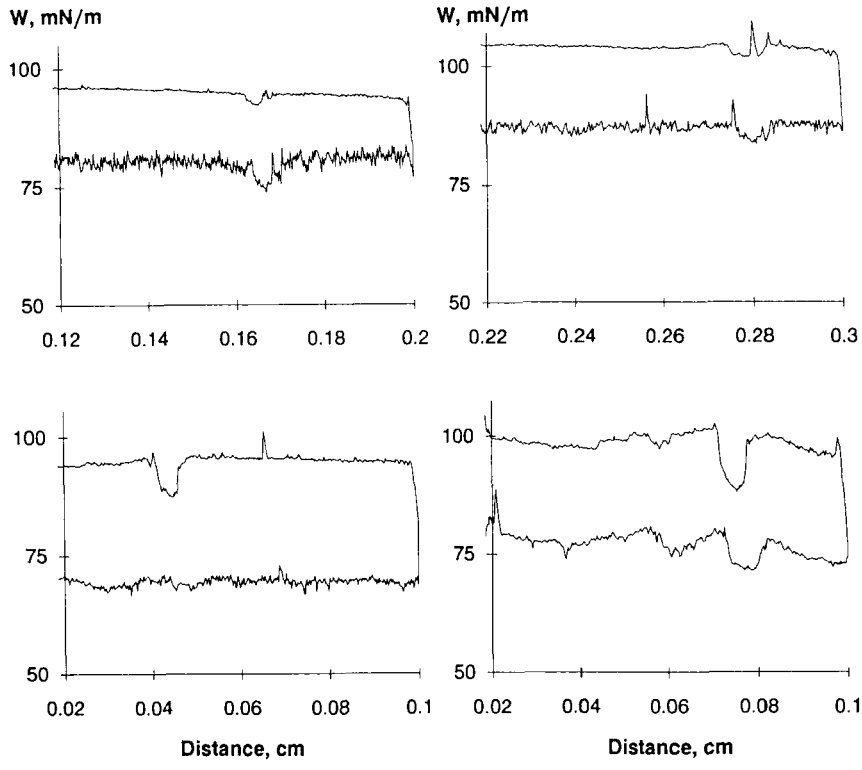

FIGURE 6 Wettability scans in the third wetting cycle for four debonded HMS/Epon828 specimens.

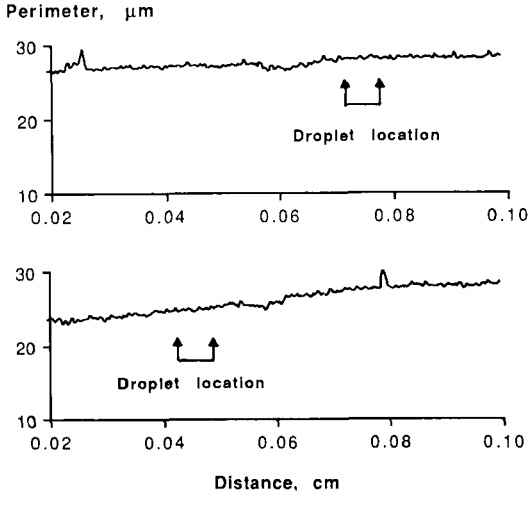

FIGURE 7 Perimeter scans of HMS fibers after debonding Epon828 microdroplets.

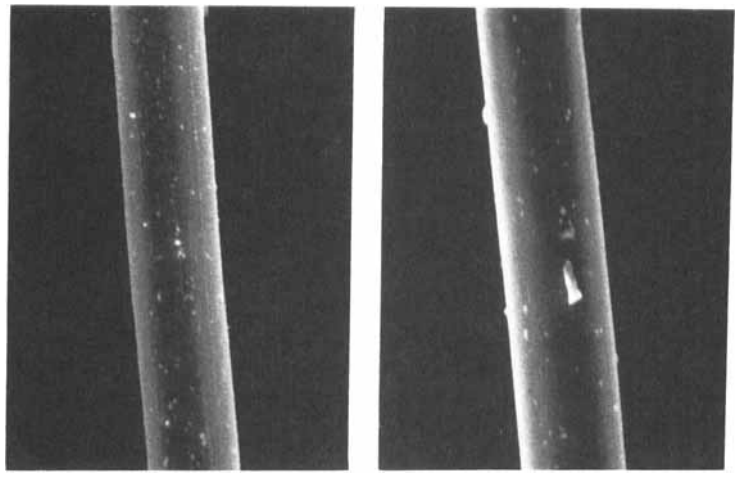

FIGURE 8 Representative SEMs of HMS fibers after debonding Epon828 droplets.

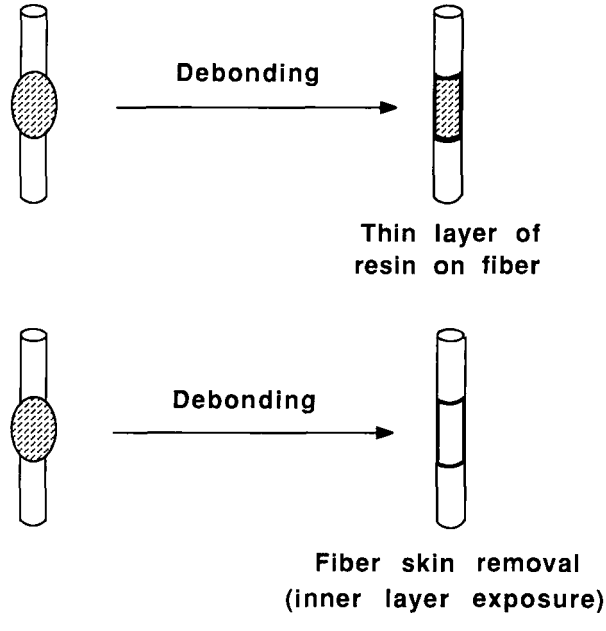

FIGURE 9 Possible fracture mechanisms for HMS/Epon828 specimen.

found to be lower than the wettability of the fiber surface, a decrease in work of adhesion at the fracture surface supports both possibilities.

To distinguish between the two modes of failure, microbond specimens were prepared in which the resin was tagged with a fluorescent probe (CIFB-113, Blankophor BA, Mobay Corp., Rock Hill, SC). The microdroplet was then debonded as before and moved away from the original site. A microfluorometric scan of a typical

debonded specimen (Figure 10, top) gave no evidence of residual resin, although the corresponding wettability scan (Figure 10, bottom) showed a decrease at the fracture surface.

This leaves us with the alternative possibility that fiber/resin debonding in HMS/epoxy involves removal of a layer of carbon fiber. The thickness of this layer would have to be less than the limits of detection of both SEM and perimeter measurements.

AS4/epoxy

This fiber/resin system exhibited various types of failure mode. Three representative wettability scans of fracture surfaces, along with their corresponding perimeter scans, are shown in Figures 11, 12, and 13. The wettability data in Figure 11 show that the surface energetics and the perimeter of the fiber along the fracture surface

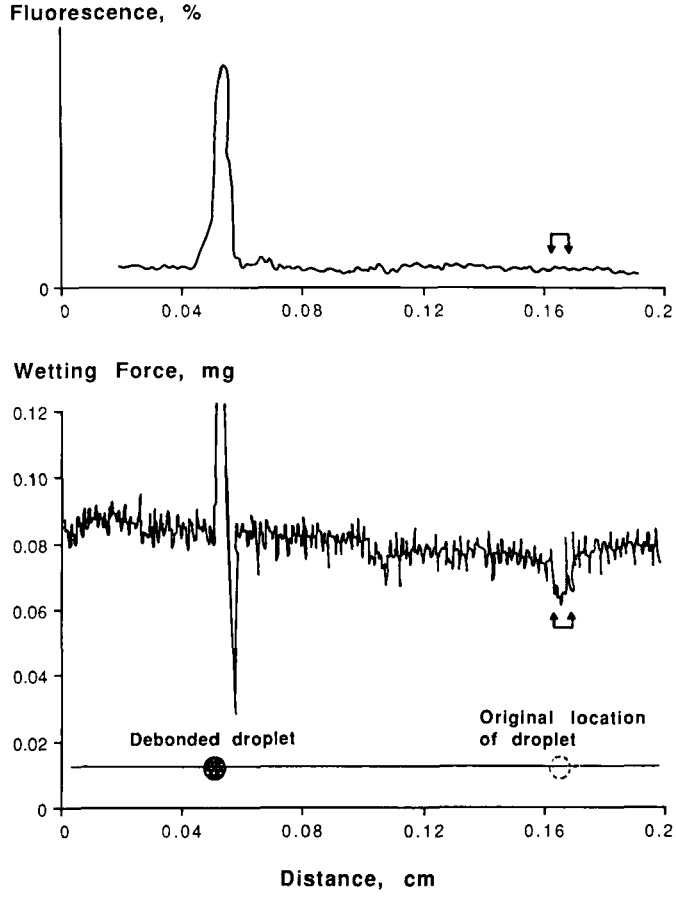

FIGURE 10 Microfluorometric (upper) and advancing wettability (bottom) scans of debonded HMS/epoxy specimen. Sharp peaks on both scans show the present droplet location. The decrease in W at the fracture surface is not associated with any change in fluorescence intensity.

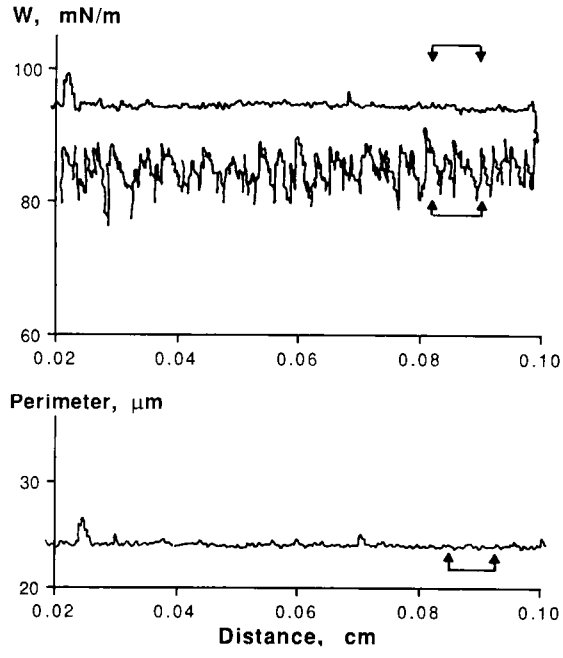

FIGURE 11 Wettability and perimeter scans of debonded AS4/epoxy specimen. No change can be detected at the fracture surface in either scan, indicating clean interfacial failure.

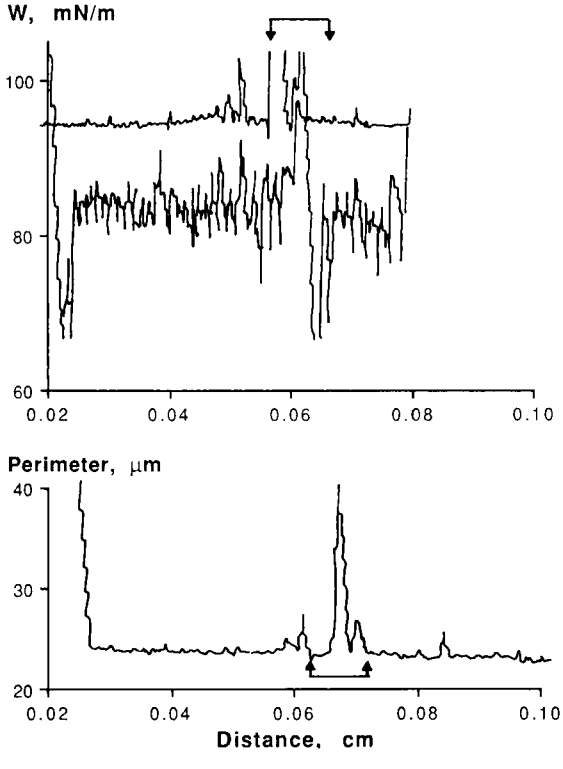

FIGURE 12 Wettability and perimeter scans of debonded AS4/epoxy specimen. An increase in W at the fracture surface is associated with a perimeter change, indicating presence of resin residue.

are identical to the rest of the fiber. This suggests a clean adhesive failure at the interface. On the other hand, the data in Figure 12 indicate that there was cohesive failure in the resin as evidenced by an increase in perimeter in the region of the fracture surface.

Some specimens showed a complex failure mechanism consisting of multiple failure modes. Wettability and perimeter scans for such a specimen are shown in Figure 13. The peaks at the two ends of the original microdroplet location indicate resin cohesive failure at the ends. Judging from the wettability and perimeter scans, the amount of resin residue closer to the fiber end is much smaller than that at the other end, probably because the debonded resin droplet, as it is pushed downward, removed most of the resin residue along its path. However, the portion of the fiber between the two regions of cohesive failure shows a well-defined decrease in wettability with no change in the fiber perimeter. This wettability drop is very similar to that observed for the HMS/epoxy system and probably reflects removal of the fiber skin.

The measured interfacial shear strength (IFSS) values for the specimens of Figures 11, 12, and 13 were 28.8, 45.9, and 39.8 MPa, respectively. These IFSS data are consistent with the failure mechanisms suggested by the wettability measurements. For a specimen with relatively low interfacial adhesion (*e.g.*, Figure 11),

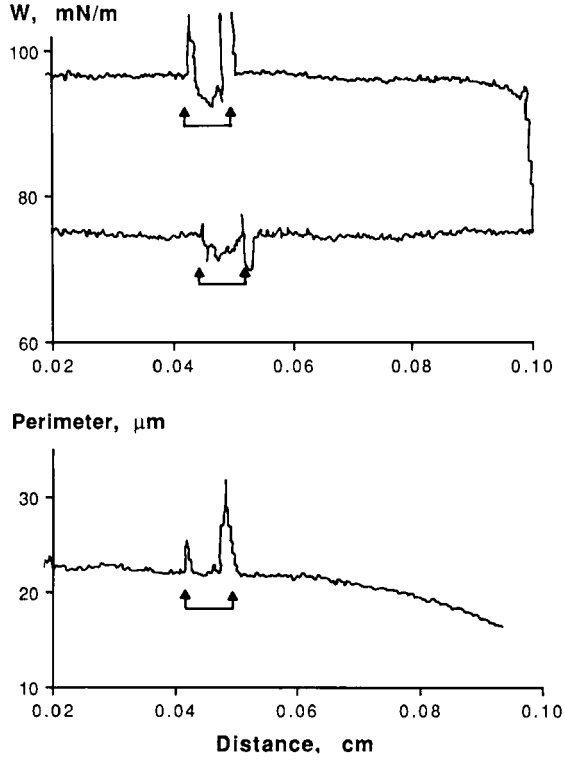

FIGURE 13 Wettability and perimeter scans of debonded AS4/epoxy specimen. Complicated failure

TABLE I
IFSS and fracture mechanisms for HMS and AS4/epoxy systems

Fiber/resin	Failure type	No. of specimens	IFSS, MPa*
HMS/epoxy	Cohesive failure in fiber—removal of fiber skin	15	29.9 ± 3.1
AS4/epoxy	Complex failure mechanisms: adhesive as well as cohesive failures in fiber and resin	17	45.6 ± 6.4

*Average ± 95% confidence.

clean adhesive failure takes place. If the interfacial adhesive strength is higher than the cohesive strength of either fiber or resin phase, however, cohesive failure will be involved in fiber/resin debonding (*e.g.*, Figures 12 and 13). It would be informative if we could find quantitative correlations between fracture mechanisms and measured IFSS, but since the failure mode may not be uniform across the interface and since we cannot determine what fraction of the interfacial area participates in cohesive failure, such correlations cannot be made at this point.

Fracture Mechanisms

The proposed failure mechanisms and the average measured IFSS for the carbon fiber reinforced composites investigated are summarized in Table I. The differences between the failure modes and IFSS values for the two systems are believed to be a consequence of the fiber structure. The three-dimensional structure of HMS fiber is composed of many graphite planes having higher axial orientation at the surface than in the core.[6] A high modulus carbon fiber requires the stiff graphite layers to be aligned approximately parallel to the fiber axis. It has been shown that high modulus fiber has a thin, highly oriented, onion-skin surface layer about 50 to 100 nm thick.[7] It is reasonable to expect that this onion-skin structure has a lower intrinsic shear strength, and debonds at lower shear strengths than those at which fiber/matrix interfacial debonding occurs. However, the graphite planes in AS4 fiber are not as oriented as in HMS fiber, suggesting a higher instrinsic shear strength; we expect, therefore, that the AS4/epoxy system should exhibit a higher IFSS and more complicated failure modes.

CONCLUSIONS

The wettability scanning technique has been shown to be very effective for studying the fracture surface between resin and carbon fiber. Various failure modes were observed in different carbon fiber reinforced composites using this technique. Fiber structure appears to be an important factor affecting the fiber/resin mechanism and the apparent interfacial shear strength.

Acknowledgment

These studies are one aspect of research on the TRI project "Adhesion and Fiber Composites," supported by a group of Corporate TRI Participants.

References

1. L. T. Drzal, M. J. Rich, and P. F. Lloyd, *J. Adhesion* **16,** 1 (1982).
2. L. T. Drzal, M. Rich, M. Koenig, and P. F. Lloyd, *J. Adhesion* **16,** 133 (1983).
3. S. Brelant, *SAMPE J.* **31,** 6 (1985).
4. B. Miller, P. Muri, and L. Rebenfeld, *Comp. Sci. Tech.* **28,** 17 (1987).
5. B. Miller, L. S. Penn, and S. Hedvat, *Colloids and Surfaces* **6,** 49 (1983).
6. R. J. Diefendorf and E. W. Tokarsky, *The Relationship of Structure to Properties in Graphite Fibers,* AFML-TR-72-133 (1977).
7. W. Ruland, *Polymer Reprints* **9,** 1368 (1968).